Behavioural Brain Research 515 (2026) 116417

Contents lists available at ScienceDirect

Behavioural Brain Research

journal homepage: www.elsevier.com/locate/bbr

Research article

Differential association of high- and low-frequency rat vocalizations with breathing and locomotion during social interactions

Yizhaq Goussha [a,*,1], Noemi Foà [b,1], Rishika Tiwari [a], Shanah Rachel John [c], Shai Netser [a], Philip Tzvi Reiss [b], Shlomo Wagner [a]

[a] Sagol Department of Neurobiology, Faculty of Natural Sciences, University of Haifa, Israel
[b] Department of Statistics, Faculty of Natural Sciences, University of Haifa, Israel
[c] Solomon H. Snyder Department of Neuroscience, Johns Hopkins University School of Medicine, Baltimore, MD 21205, USA

ARTICLE INFO

Keywords:
Rat ultrasonic vocalizations
Low-frequency vocalizations
Breathing patterns
Social interactions
Machine learning
Semiparametric mixed-effects models
Theta rhythmicity

ABSTRACT

Rodents, including rats, utilize vocalizations as a primary mode of social communication. While high-frequency ultrasonic vocalizations (USVs) have been extensively explored in laboratory rats, low-frequency (<10 kHz) vocalizations (LFVs) were first described only recently, and it is as yet unclear whether these two types of vocalizations are driven by the same behavioral mechanisms. This study investigates the behavioral distinctions between USVs and LFVs in socially interacting rats. In line with previous studies, we found that USVs, mostly associated with social interactions, are emitted during early stages of exhalation and involve complex respiratory modulations. In contrast, LFVs, which correlate with general arousal, occur early at inhalation, show limited deviation from baseline breathing patterns, and are significantly associated with locomotion. Advanced machine learning models, including long short-term memory convolutional neural network frameworks and semiparametric mixed-effects models, were employed to analyze the interplay between vocalizations, respiration, body orientation and locomotion. The results of these analyses demonstrate that USVs are well predicted by the breathing pattern and are associated with social interaction and orientation toward the social stimulus. In contrast, LFVs were predicted poorly from the breathing pattern alone, but are correlated with both breathing rate and locomotion. Moreover, they shared common dynamics with the power of theta oscillations in the nucleus accumbens core, a brain area associated with motivation and emotions. We conclude that these two vocalization types represent distinct communicative and physiological phenomena. These findings advance the understanding of rodent vocal communication and highlight the possible adaptive roles of LFVs in behavioral contexts.

1. Introduction

1.1. Animal vocal communication

Vocal communication is a fundamental component of social behavior across the animal kingdom, enabling individuals to influence conspecifics and exchange information about both the external environment and their internal state [1]. At one end of this communicative spectrum are highly specific, intentional-like vocal signals that convey information about external referents, exemplified by the alarm calls of vervet monkeys, which elicit predator-specific responses in listeners and are often described as functionally referential calls [2–4]. At the other end are vocalizations that are more directly shaped by the sender's affective state, such as distress cries, screams, or laughter, which primarily communicate emotional arousal, valence, or motivation rather than a discrete external referent [5,6].

1.2. Rodent vocalizations

Rodents, particularly rats, rely on vocalizations for social communication [7]. These vocalizations, many of which are ultrasonic (>20 kHz), beyond the range of human hearing, play an important role in signalling emotional states and social intentions [8]. Adult rats primarily produce two main types of ultrasonic vocalizations (USVs):

* Corresponding author.
E-mail address: ygoussha@campus.haifa.ac.il (Y. Goussha).
[1] These authors contributed equally to this work

https://doi.org/10.1016/j.bbr.2026.116417
Received 31 July 2025; Received in revised form 10 July 2026; Accepted 6 August 2026
Available online 7 August 2026

50-kHz calls, largely associated with positive social interactions such as mating or play, and 22-kHz calls, typically linked to negative emotional states such as distress or alarm [9–11].

1.3. Respiration dynamics and their association with rat vocalizations

While vocalizations provide valuable information on rodent emotional states, they are not the only indicator of internal states in these animals. Another crucial yet often overlooked aspect of rodent physiology that reflects their state is their respiratory patterns (also termed "breathing" or "sniffing"). The rate and depth of breathing can fluctuate rapidly in response to external stimuli, social interactions, cognitive tasks, and internal states [12–15].

Notably, respiration has been shown to play a pivotal role in structuring rat USVs. Active sniffing, characterized by rhythmic breathing at 5–15 Hz (theta rhythmicity), is tightly coupled with the emission of 50-kHz USVs, which occur during the exhalation phase and prolong the respiratory cycle [16]. This dynamic coordination links respiratory control to neural circuits governing communication [17].

1.4. Detecting low-frequency rat vocalizations during social behavior

Studying rodent vocalizations, especially during social interactions involving multiple animals, presents significant challenges due to the difficulty of reliably attributing specific vocalizations to individual animals. To address this, in a previous study [18] we developed a novel method for simultaneous recording of both breathing and vocalizations from individual rats. This method utilizes two microphones: a miniature microphone attached to the nasal cavity via an implanted cannula connected to a flexible tube, and an arena microphone placed above the arena. The miniature microphone captured the subject's vocalizations and breathing activity, while the arena microphone recorded all USVs produced within the experimental arena. This dual microphone system allowed us to separate vocalizations from different rats during restricted and free social interactions, even in close proximity. Using this technique, we revealed a novel, *low-frequency* (4–10 kHz) type of vocalizations (LFVs), which appear to represent a distinct form of rat vocalization. We also demonstrated that, unlike USVs, the rate of LFVs rose before stimulus introduction, like the breathing rate, thus suggesting a relation to an increased arousal state induced by the expectation of a social encounter. Notably, LFVs were evidently too weak to be detected by the more distant arena microphone, but were captured clearly by the miniature microphone attached to the subject's nasal cavity.

1.5. Summary of the results of the current study

In the current study, we conducted a detailed analysis comparing the breathing patterns recorded during USVs and LFVs with silent breathing (SB) periods without any vocalizations. Our results indicate that breathing patterns associated with LFVs are more similar to SB, whereas breathing patterns during USV emissions were accompanied by noticeable deviations from SB patterns.

We further investigated the dynamics of rat vocalizations and their relationship to breathing using a hybrid long short-term memory-convolutional neural network (LSTM-CNN) model. The LSTM-CNN model was employed to detect vocalizations using breathing patterns. This approach successfully detected USVs, as the breathing patterns changed significantly during their emission. However, the model struggled to detect LFVs from the breathing patterns alone, as these patterns showed little deviation from SB patterns when LFVs were emitted.

In addition, we modelled the rate of USVs and LFVs as a function of breathing rhythm, animal speed, body orientation and social behaviour using semiparametric negative binomial mixed-effects models [19], which model linear and nonlinear effects while accommodating the hierarchical structure of repeated measurements across multiple trials. These models yielded contrasting results for USVs versus LFVs. Specifically, animals' speed was found to be a significant predictor exclusively for LFVs, while social interaction and body orientation toward a social stimulus were associated with USVs.

Finally, we analyzed the temporal and spatial association of each vocalization type and found a significant association between USVs and the social stimulus's location and vocalizations, while LFVs were specifically associated with increased local field potential (LFP) theta power in the nucleus accumbens.

Overall, our results suggest that USVs and LFVs play distinct functions, with USVs closely tied to social interactions and LFVs reflecting broader internal states.

2. Methods

2.1. Animals

Subject animals were Sprague-Dawley (SD) adult rats (9–15 weeks of age, 300–450 g), while SD male and female rats (5–6 weeks, 250–300 g) served as stimuli. For vocalization and breathing recordings 8 males and 4 females were used as subjects (with male and female stimuli), while for electrophysiological recordings we used 10 males as subjects (with male stimuli only). All rats were grown in-house and were kept in the animal facility of the University of Haifa under veterinary supervision, with *ad libitum* access to food and water, 23 °C temperature, and 60% humidity. Rats were housed in groups of 2–5 animals per cage (60x40x20 cm), depending on age, under a 12-h light/12-h dark cycle, lights on at 7 p.m. Behavioral experiments took place during the dark phase of the cycle, under dim red light. All experiments were performed according to the US National Institutes of Health guidelines for the care and use of laboratory animals and with approval by the Animal Care and Use Committee (IACUC) of the University of Haifa.

2.2. Experimental setup and design

This study builds upon our previous paper [18], where all experimental details are described. To record vocalizations during social interactions, we employed the social preference (SP) test, in which subject animals are exposed to social (a conspecific) and object (plastic toy, ~5 ×5 cm) stimuli simultaneously [20]. The experimental setup (see Fig. 1) consists of an arena (50 ×50 ×40 cm) made of black Plexiglas, placed inside an acoustic chamber that was illuminated by dim red LED lights. For electrophysiological recordings, this acoustic chamber was electrically shielded with metal aluminum plates. The arena contained two triangular Plexiglas chambers (21 ×21 ×40 cm) in opposite corners with metal mesh at their sides facing the arena to allow a direct interaction between the subject and the stimulus through the mesh.

The social preference (SP) test session started with a 15-minute habituation to the arena containing two empty chambers. During this time, stimulus animals were placed in other chambers for acclimation. The recording session started with a 5-minute baseline recording (pre-encounter phase). Thereafter, the empty chambers were replaced with the animal and object stimulus chambers, and the SP task was performed for 5 min (encounter phase). Following the task, the chambers with the stimuli were replaced with empty chambers, and the subject rat was recorded for an additional 5-minute period (post-encounter phase).

2.3. Electrophysiological recordings

The recorded animals were implanted with custom-made electrode arrays as previously described [21], using the following coordinates for the nucleus accumbens core: A/P = + 2 mm, L/M = ±1.4 mm, D/V = −7.1 mm. Behavioral experiments were conducted as described above and recordings were obtained as previously described [22].

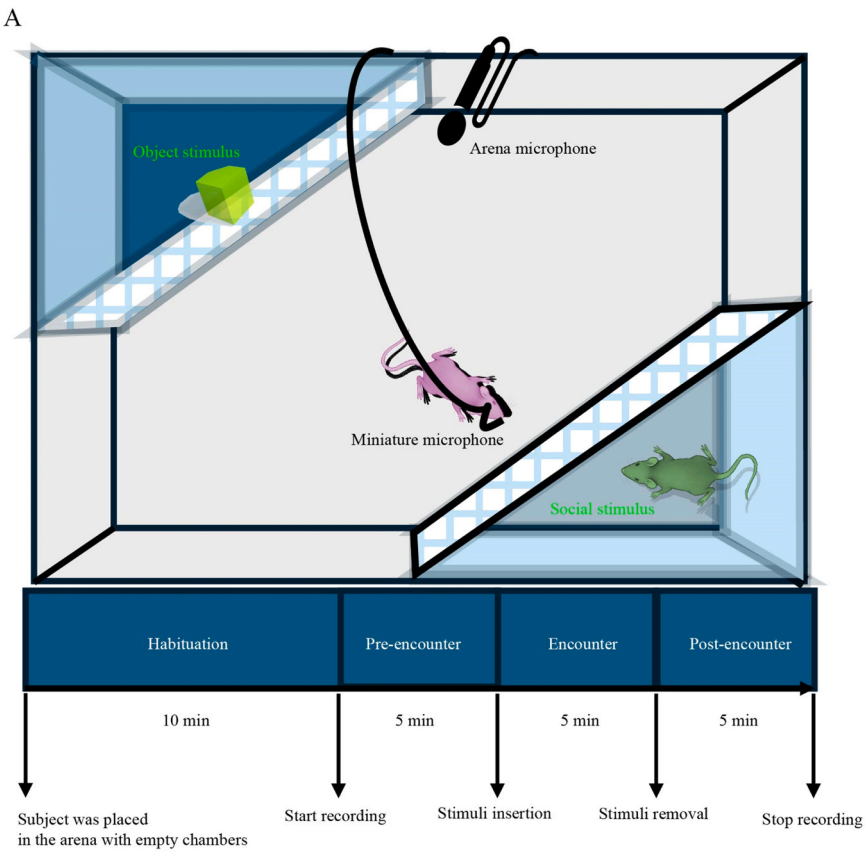

Fig. 1. Experimental design and timeline. Social preference assay and recording protocol. A 50 × 50 × 40 cm Plexiglas arena held two triangular mesh chambers that could house either an object or a stimulus rat; the freely moving subject rat wore a nasal miniature microphone while an overhead arena microphone captured all sounds. Empty chambers were present during the 15-minute habituation + pre-encounter period, replaced by object and stimulus chambers for a 5-minute encounter, then reinstated for a 5-minute post-encounter recording, as summarized in the timeline.

2.4. Data acquisition and annotation

A dual-microphone system was used to record the subject rats' breathing and vocalizations (USVs and LFVs) during social interactions. Each subject rat was equipped with a miniature microphone connected to an implanted cannula in its nasal cavity via a short polyethylene tube, which captured breathing activity and vocalizations. An arena microphone positioned above the cage recorded vocalizations from both the subject and stimulus rats, while a video camera captured the subject's behavior. For full experimental details, see [18]. This strategy allowed us to identify which USVs are emitted by the subject (detected by both microphones) and which are emitted by the stimulus animal (detected only by the arena microphone). It also enabled the detection of LFVs, which were too weak to be detected by the more distant arena microphone, but were captured clearly by the miniature microphone attached to the subject's nasal cavity.

2.5. Behavioral analysis

The subject's behavior was analysed from the recorded video clips using TrackRodent software (https://github.com/shainetser/TrackRodent) [20], with the *WhiteRatWiredHeadDirectBased* algorithm tracking the subject's movement in the arena. This analysis was used to determine the investigation behavior and speed of the animal. Other behavioral analyses were done using DeepLabCut [23] as described below.

2.5.1. Subject rat pose estimation using DeepLabCut

DeepLabCut (DLC) version 2.3.8 [23] was applied for single animal pose estimation. Eight anatomical landmarks were annotated: the left ear, right ear, nose, neck, trunk, the two lateral sides of the body, and the tail base. Only the neck and trunk coordinates were included in the downstream analyses.

A total of 800 frames from four videos of SD rats were manually labeled. Training used a dlcrnetms5 network with default settings and two million iterations. An outlier-refinement stage was performed to improve prediction quality. The final model achieved a test error of 5.5 pixels and a training error of 4.42 pixels. The trained network was subsequently applied to all remaining recordings.

2.5.2. Subject body orientation analysis

For each frame, the XY coordinates of the trunk and neck were obtained using our trained DLC model. The animal's heading vector v was defined as the difference between neck and trunk positions, and the line of sight to the stimulus or object chamber was defined as the vector w from the neck to the centroid of the corresponding chamber as defined by the TrackRodent software. The angle θ between these two vectors was derived from the dot product formula

$$\cos\theta = \frac{v \bullet w}{\|v\|\|w\|}.$$

Angles were expressed in degrees and then shifted by subtracting

ninety degrees so that −90° corresponds to the subject facing the social chamber, + 90° corresponds to facing the object chamber, and 0° indicates a perpendicular body orientation. Frames containing at least one landmark with DeepLabCut confidence below 0.6 were excluded, and angles were aligned to stimulus insertion events and binned in half-second intervals for subsequent analysis.

2.5.3. Spatial localization of vocalizations

To determine the spatial position of the subject at the moment of vocalization, mid of trunk-neck coordinates obtained from DeepLabCut tracking were used as the animal's instantaneous location. Vocalization onset times from the HybridMouse annotations (see below) were matched to the nearest video frame, and the mid of trunk-neck coordinates at that frame was assigned to the event.

Because arena orientation differed across sessions, coordinates were standardized before pooling the data from all sessions. For each recording, the centroid of the social stimulus chamber polygon was computed, and the entire coordinate system was rotated in multiples of 90° until the social chamber occupied a common reference corner. The same transformation was applied to all tracked positions. Spatial heat maps were then constructed in this normalized frame by binning positions into two-dimensional histograms. Separate maps were generated for USV emission sites, LFV emission sites, and overall subject occupancy across time. Distances from the social stimulus were calculated as Euclidean distances between event locations and the centroid of the rotated chamber polygon.

2.6. Vocalization and breathing analysis

Audio signals sampled at 250 kHz were analysed using the HybridMouse system, as previously described [24]. A pre-trained deep neural network identifying all USVs was followed by an observer who validated these results, marked each USV on a spectrogram, and identified all LFVs.

2.6.1. Breathing cycle segmentation and labeling

Breathing cycles were segmented from the miniature microphone signal using a morphology-based procedure designed to identify the landmarks of transition between inhalation and exhalation. The raw breathing trace was first downsampled to 5 kHz and detrended to overcome a certain instability of the miniature microphone signal, caused by its high sensitivity. The detrended signal was then smoothed by MATLAB's *smooth* function, to produce a smoothed trace (Fig. 2B), which was convolved with a representative breathing-cycle template. Candidate upper extrema were then detected on this convolved trace using the function *findpeaks* (with parameter mindist=500 samples) and

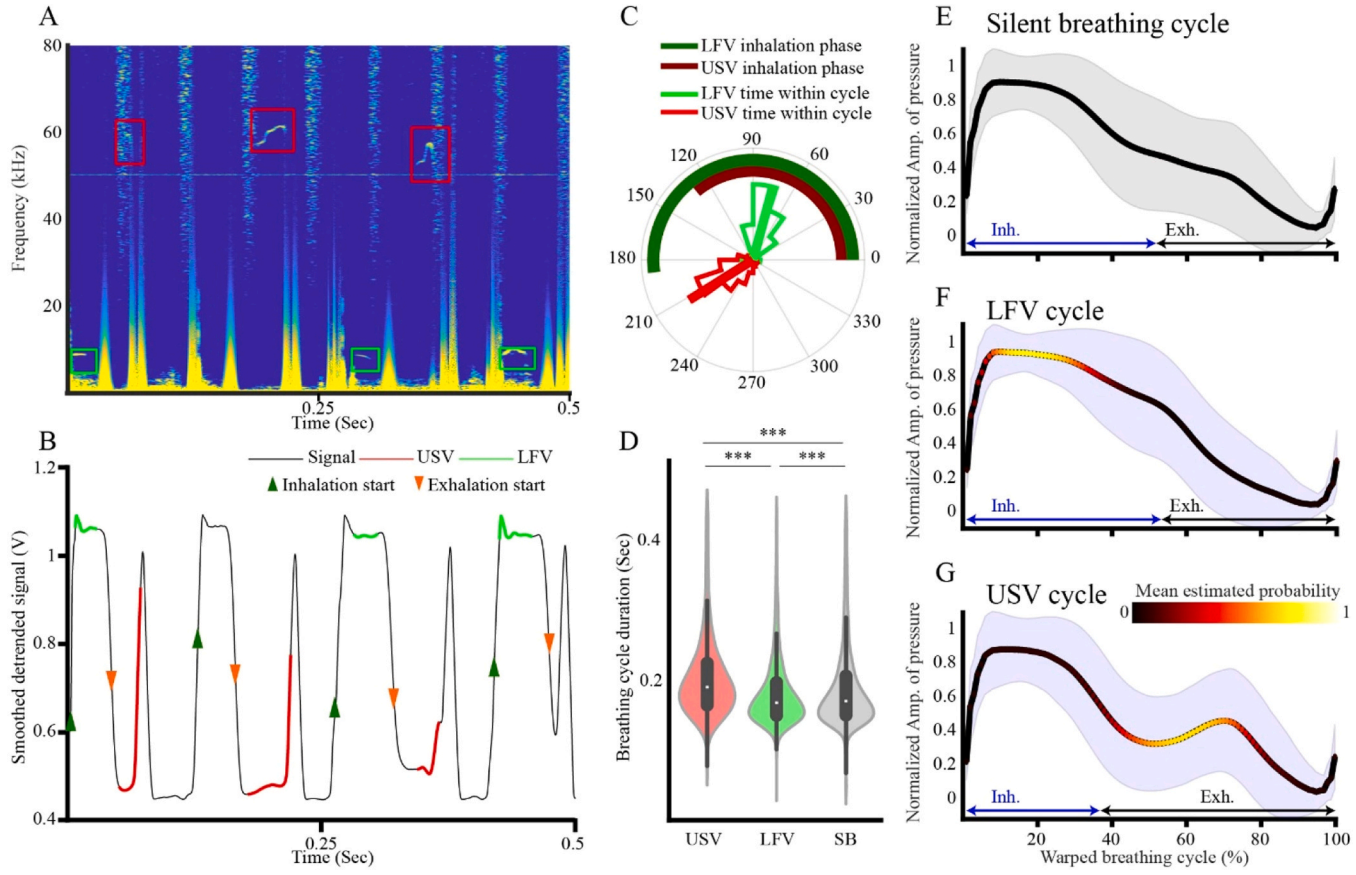

Fig. 2. Spectro-temporal features of USV and LFV emissions in relation to breathing patterns. (A) Example spectrogram recorded from the nasal miniature microphone, with color-coded signal power. USVs are highlighted by red boxes and LFVs by green boxes. (B) A smoothed detrended signal trace corresponding to A, with USV-containing periods marked in red and LFV-containing periods in green, illustrating their timing relative to the breathing cycles. Arrowheads mark the inhalation (green) and exhalation (orange) starting times. (C) Polar histogram of vocalization center within the normalized breathing cycle. LFVs are shown in green and USVs in red. Radial lines indicate the circular mean and histogram of the center for each vocalization type, and the outer arcs indicate the median inhalation span estimated separately for LFV- and USV-containing cycles. (D) Distribution of breathing-cycle durations for silent breathing (SB) cycles, LFV-containing cycles, and USV-containing cycles. Asterisks indicate significant differences, $p < .001$ (independent samples t-test, corrected for multiple comparisons). *(E-G)* Mean normalized breathing-cycle profiles for silent breathing, LFV-containing, and USV-containing cycles, respectively. Shaded regions indicate variability across cycles. In panels *F* and *G*, line color represents the estimated probability of the corresponding vocalization type across the normalized (resampled) breathing cycle. Inhalation and exhalation phases are denoted below.

a threshold of 0.3 (a.u.). For each upper extremum, the corresponding lower extremum was defined as the minimum signal value occurring between the preceding and current upper extremum. See deposited code for more details.

Because the miniature microphone signal reflects nasal pressure changes rather than absolute pressure, phase transitions were not defined by a fixed amplitude threshold or zero crossing. Instead, transition landmarks were identified from the slope of the smoothed detrended signal. For each lower-to-upper extrema interval, corresponding to the rising portion of the cycle, inhalation starting time was defined as the point of maximal positive slope within the first major rising segment. To distinguish the primary rising segment from small local fluctuations, positive derivative magnitudes within each interval were separated into weak and steep slope regimes using an Otsu-based adaptive threshold [25], and the earliest contiguous steep positive-slope segment was retained.

Exhalation starting time was determined analogously, but with an additional constraint to account for vocalization-related waveform distortions. Due to the miniature microphone high sensitivity, rat vocalizations could introduce a secondary rise-and-fall deflection during the exhalation phase of the waveform (Fig. 2B). Therefore, for each upper-to-lower-extrema interval, negative derivative magnitudes were separated into weak and steep slope regimes using the same Otsu-based adaptive threshold as above, and the exhalation starting time was defined as the point of maximal negative slope within the first major descending segment following the upper extremum. This procedure targeted the initial plateau-to-drop transition while avoiding later negative-slope events associated with intra-expiratory waveform perturbations.

A breathing cycle was then defined from one inhalation start time to the subsequent inhalation start time. Within each cycle, the inhalation phase extended from the cycle start time to the detected exhalation start time, and the exhalation phase extended from the exhalation start time to the onset of the next cycle. Cycles with strongly atypical durations (z-score>1) were excluded before further analysis. Each retained breathing cycle was normalized between 0 and 1 and resampled to a standardized length of 100 bins using the *resample* MATLAB function. Each breathing cycle was then labeled as containing a USV, LFV, or as silent breathing (SB). In order to identify the vocalization timing within each cycle, logical vocalization vectors (binary representation of the time bins containing each vocalization) were segmented using the same cycle boundaries and resampled to the same 100-bin representation. We then averaged across cycles to obtain, for each vocalization type (USV and LFV), the empirical probability of vocalization within each of the 100 time bins (Fig. 2E-G).

2.6.2. Dynamic time warping analysis

Dynamic time warping (DTW) is a non-linear alignment procedure that computes the minimal cumulative cost required to match two sequences by locally stretching or compressing their time axes so that similar patterns coincide [26]. Each vocalization-bearing breathing cycle was represented as $X = \{x_1, x_2, \ldots, x_n\}$, and compared with the mean silent-breathing (SB) template $Y = \{y_1, y_2, \ldots, y_m\}$, which was obtained by averaging all SB segments. The DTW distance d(X,Y) was obtained with MATLAB's *dtw* function (Signal Processing Toolbox), which implements the dynamic-programming recursion introduced by Sakoe and Chiba [27]. These distances were pooled across animals and compared among USV, LFV, and SB cycles using a one-way ANOVA, followed by Bonferroni-corrected pairwise comparisons.

2.6.3. Cross-vocalization probability analysis

To quantify the temporal synchronization between vocalization types, we calculated the conditional probability of a target vocalization occurring within a 5-second window centered on a reference vocalization. Data were pooled across all sessions to compute a single global probability, defined as the total count of reference events containing at least one concurrent target event divided by the total number of reference events. Uncertainty for these probability estimates was quantified using 95% binomial confidence intervals. To assess statistical significance, we performed a Monte Carlo permutation test (with 1000 iterations) using a circular shift procedure. In each iteration, the timestamps of the target vocalization series were circularly shifted by a random offset within the session duration. This approach preserved the internal temporal structure (e.g., inter-event intervals and burstiness) and total count of the target series while destroying its specific temporal alignment with the reference vocalizations. P-values were calculated as the proportion of surrogate iterations where the overlap probability met or exceeded the observed value.

2.6.4. Circular analysis of vocalization onset timing

To quantify the phase tendency of vocalization onset within the respiratory cycle, we extracted the first time bin in which a vocalization occurred for each USV- and LFV-labeled normalized 100 bin breathing cycle. These onset bins were then converted to angular phase values on the interval $[0, 2\pi]$ radians using the transformation $\theta = 2\pi \cdot (b - 1)/100$, where b is the bin number. We computed the mean direction, resultant vector length, and performed Rayleigh's test to assess non-uniformity in the phase distributions. A Watson–Williams test [28] was used to compare the mean onset phases between USVs and LFVs. All circular analyses were performed using the Circular Statistics Toolbox for MATLAB.

2.7. LSTM-CNN model training and testing

We developed a bidirectional long short-term memory convolutional neural network (BiLSTM-CNN) model utilizing an eight-layer residual network (ResNet) [29] as the backbone.

2.7.1. Input preprocessing

Recordings were down-sampled from 250 kHz to 1 kHz. The 1D audio vector was reshaped into an overlapping 2D matrix with dimensions $(\text{Win} \times N_{\text{hops}})$, where:

$$N_{\text{hops}} = \left\lfloor \frac{m - \text{Overlap}}{\text{Win} - \text{Overlap}} \right\rfloor$$

with m as the number of bins in the down-sampled vector, Win $(= 500)$ as the output length in bins, and Overlap $(= 130)$ as the overlap length in bins.

Continuous wavelet transformation (CWT) was performed using the MATLAB Wavelet Toolbox's *cwt* function, with a filter bank configured to extract time-frequency characteristics from breathing waveforms. The transformation was applied using 10 voices per octave to achieve fine spectral resolution, with the analytic Morse wavelet used as the basis function. The sampling frequency was set to 1 kHz, and the signal length was fixed at 2000 bins to ensure consistency across cycles. The time bandwidth parameter was set to 60, balancing time and frequency localization, and boundary effects were mitigated using signal reflection. CWT was applied to segments of length $Win = 500$ bins, with an overlap = 130 bins between windows. The number of bins in each down-sampled vector is denoted by m. This transformation converts each audio vector into a feature matrix with 81 extracted features. The absolute values of these feature matrices were centered, resulting in final input dimensions of $81 \times 500 \times 1 \times N_{\text{hops}}$.

2.7.2. Model evaluation

The dataset was divided into training and validation sets with an 80%/20% split. To assess generalization across subjects, all recordings from one rat were held out and used exclusively as the test set.

The performance of the BiLSTM-CNN model was evaluated using the

F1 score, which is the harmonic mean of precision and recall, providing a balanced measure of the model's classification accuracy; formally, $F1 = 2 \times \frac{\text{Precision} \times \text{Recall}}{\text{Precision} + \text{Recall}}$, where precision is defined as $\frac{TP}{TP+FP}$ and recall is defined as $\frac{TP}{TP+FN}$, with $TP, FP,$ and FN representing true positives, false positives, and false negatives, respectively.

2.8. Semiparametric negative binomial mixed-effects models

We used advanced count regression to model the relationship between the number of vocalizations (USVs or LFVs) within each half-second interval and several predictor variables. The response variable, number of vocalizations, ranged from 0-4 for USVs and 0–5 for LFVs. The predictor variables were as follows:

1. The rodent's speed, in number of pixels travelled per 0.5-s time bin. This ranged from 0 to 286 pixels, and was found to be strongly right skewed. To mitigate this, a logarithmic transformation was applied; the log speed ranged from -4.29 to 5.11.
2. Breathing rate, which ranged from 0 to 13 Hz.
3. Which of five "states" the subject rat was in during the given half-second bin, where the states were defined as (i) pre-encounter, (ii) post-encounter, and three mutually exclusive states during the encounter phase: (iii) touching the social stimulus, (iv) touching the object, and (v) touching neither.

This analysis includes data from a total of 19 unique experiments involving 8 rats (4 males and 4 females). In total, the dataset has 11419 half-second time bins, of which 2372 were excluded due to missing values of the animal's speed (due to occlusion during the introduction and removal of the stimuli). The numbers of time bins in each state are detailed in Table 1 below.

The regression models were *semiparametric negative binomial mixed-effect models*. Here the term *semiparametric* refers to the fact that the model combines ordinary (parametric) effects of state along with smooth nonlinear (nonparametric) functions of log speed and breathing rate, as detailed in the formal model statement below. The *negative binomial* distribution is an alternative to the Poisson, the standard distribution for a count response (in our case, the number of vocalizations in each half-second). Whereas the Poisson distribution assumes the variance to be equal to the mean, our data appear to have variance exceeding the mean (overdispersion), which the negative binomial distribution accommodates by incorporating, alongside the mean μ, a second parameter θ (see below). *Mixed-effect* refers to the fact that the model includes both fixed effects of the above predictors and random effects of trial, to take into account the nesting of observations (half-seconds) within trial.

Formally, the model for each vocalization type is

$$Y_i \sim \mathrm{NB}(\mu_i, \theta),$$

$$\log(\mu_i) = \beta_0 + \tau_{state(i)} + \quad f_1(\log(\text{speed})_i) + f_2(\text{breathing}_i) + b_{trial(i)}$$

where:

- Y_i is the number of vocalizations (USV or LFV) in the i^{th} observation (half-second interval);
- $\mathrm{NB}(\mu_i, \theta)$ is the negative binomial distribution with mean μ_i and a second parameter θ such that $Var(Y_i) = \mu_i + \mu_i^2/\theta$;
- $\tau_{state(i)}$ is the effect of the state the rat is in during the i^{th} observation;
- f_1, f_2 are smooth functions, modeled using B-splines [19], that capture non-linear effects of the continuous predictors log speed and breathing rate, respectively;
- $b_{trial(i)}$ is a zero-mean, normally distributed random effect of the trial within which the i^{th} observation occurs.

Table 1
Number of 0.5-s time bins in each of the five states.

State	Frequency
Pre-encounter	5960
Touching social stimulus during encounter	5849
Touching object during encounter	543
Touching neither during encounter	5628
Post-encounter	5987

In addition, for each vocalization type, we fitted a model with a predictor representing the orientation of the rat, expressed as an angle between −90° (facing the social stimulus) and + 90° (facing the object), and its interaction with state. From this interaction model we derived an angle effect for each state. This interaction model was fitted for only the three "during encounter" states, on the assumption that orientation before and after the encounter is not meaningful.

2.9. Electrophysiological analysis

As previously described [22].

2.10. Software

Signal processing and analysis steps were performed using MATLAB R2021a (The MathWorks Inc., Natick, MA, USA). Semiparametric mixed models were fitted using the *mgcv* package [30] for R, and plotted using the *mgcViz* package [31].

2.11. Data and code availability

All codes and processed data used for this paper are available in Zenodo (10.5281/zenodo.18495760).

3. Results

3.1. Comparison of vocalizations and breathing patterns

We analyzed breathing cycles from 32 social preference sessions (see Methods) in 12 rats, classifying each cycle as containing a USV, an LFV, or no vocalization (silent breathing, SB). We found temporal dissociation between LFVs and USVs within the breathing cycle (Fig. 2A–B). LFVs were typically located within the inhalation phase, while, in agreement with previous work [16,17], USVs consistently occurred during exhalation. Accordingly, circular histograms of vocal-onset timing within the normalized breathing cycle demonstrated distinct phase tendency for the two call types (Fig. 2C), with LFVs locked to the first half of the inhalation phase (mean vector =75°, resultant length =.74), whereas USVs dispersed around the first half of exhalation (mean vector = 212°, resultant length =.67). Rayleigh tests showed that both phase distributions were highly non-uniform (LFVs: $Z = 1274$, $p < .001$; USVs: $Z = 1199$, $p < .001$). A Watson–Williams test showed that their mean peak phase differed decisively, $F(1, 4991) = 8885$, $p < .001$.

Next, we calculated the duration of each type of breathing cycle (Fig. 2D). Mean ± SD cycle durations were 182.6 ± 63.1 ms for USV cycles, 159.1 ± 54.2 ms for LFV cycles, and 166.4 ± 66.5 ms for SB cycles. Holm-corrected Welch's independent-samples *t*-tests showed that USV cycles were significantly longer than both LFV cycles ($t_{4990.83} = 14.13$, $p < .001$, 95% CI [20.2, 26.7] ms, Hedges' $g = 0.40$) and SB cycles ($t_{3158.36} = 12.78$, $p < .001$, 95% CI [13.8, 18.7] ms, Hedges' $g = 0.25$). LFV cycles were also significantly shorter than SB cycles ($t_{2802.41} = -6.11$, $p < .001$, 95% CI [−9.5, −4.9] ms, Hedges' $g = -0.11$). Thus, USVs were associated with breathing-cycle lengthening, whereas LFVs were associated with a slight reduction in cycle duration relative to silent breathing.

As apparent in Fig. 2E-F, the mean waveform of LFV cycles closely

resembled that of SB cycles, displaying a relatively smooth profile. In contrast, USV cycles exhibited a characteristic secondary elevation during the latter half of the respiratory cycle (Fig. 2G). To quantify these differences in respiratory trajectory, we applied dynamic time warping (DTW) to compare individual USV, LFV, and SB cycles with the SB template. A one-way ANOVA revealed a significant difference in DTW distance among the three cycle types ($F_{2,\ 39{,}413} = 1172.3$, $p < .001$). Bonferroni-corrected pairwise comparisons showed that DTW distances were significantly greater for USV cycles than for both LFV cycles (mean difference = 3.24, 95% CI [2.99, 3.49], $p < .001$) and SB cycles (mean difference = 3.56, 95% CI [3.38, 3.73], $p < .001$). LFV cycles also had slightly greater DTW distances than SB cycles (mean difference = 0.32, 95% CI [0.13, 0.50], $p < .001$). Thus, both vocalization types were associated with changes in the respiratory trajectory relative to silent breathing, but these changes were substantially more pronounced during USVs. These findings indicate that USVs and LFVs differ not only in their timing within the respiratory cycle, but also in the extent to which their production is associated with modification of the breathing waveform.

3.2. Prediction of vocalizations from breathing patterns

Having established differences between breathing patterns containing LFVs, USVs, and SB, our next aim was to test whether USV emissions could be reliably predicted using only breathing patterns, without audio data. In a previous work [24], we developed a robust LSTM-CNN-based model that accurately identifies and extracts USVs from audio recordings. For this study, we adopted a similar LSTM-CNN approach and trained a model (Supplementary Figure 1) to detect USVs based solely on breathing patterns.

To ensure that no residual audio information was present in the breathing signals, we down-sampled the original recordings from 250 kHz to 1 kHz. This procedure removed any potential influence of ultrasonic audio signals and left only the breathing data for the model to rely on. After training, the model demonstrated strong performance in detecting USVs purely from breathing patterns. As shown in Table 2, the model achieved an F1 score of 0.744, with high precision (0.657) and recall (0.857) values.

The same LSTM-CNN-based model, now trained to detect LFVs, performed worse, achieving an F1 score of only 0.394. This poor performance can be attributed to the high similarity between LFV-containing and SB segments. These results further support our above-mentioned findings that LFVs are less disruptive to the natural breathing rhythm compared to USVs and further suggest that the two vocalization types are driven by distinct physiological mechanisms.

3.3. Semiparametric mixed-effect model results

Here we present the results of the semiparametric negative binomial mixed-effect models described in Section 2.8. In Fig. 3 the response variables (USV and LFV counts) and continuous predictor variables (speed, breathing rate and body orientation of the subject relative to the stimulus's chamber) are plotted against time. Among other patterns, these plots indicate that USVs in particular occur mainly during the social encounter, while LFVs appear before stimulus insertion and tend to stay for a while after stimulus removal. This pattern will be further analyzed below.

Table 3 shows the parameter estimates for the model defined in Section 2.8. The first estimate in each column, shown without a p-value, is the intercept β_0. This is followed by the effects $\tau_{state(i)}$ of each state relative to pre-encounter, the baseline state. Thus, for example, while touching the social stimulus during the encounter, the log expected number of USVs is higher by 2.827, relative to pre-encounter. The results indicate higher rates of USVs during and after the encounter compared to baseline, especially during the encounter when the subject rat is not touching the object. The effects of state on LFVs are much weaker: in particular, the effect on LFVs while the subject rat is touching the social stimulus is not significant.

Fig. 4 displays the functions f_1 and f_2 representing, respectively, smooth nonlinear effects of speed and of breathing rate. In contrast to the parametric results, these nonparametric model terms show stronger effects for LFVs (Fig. 4C,D) than for USVs Fig. 4A,B). The LFV effects are clearly positive. The effect of speed on LFV counts appears to plateau at moderate speed values, demonstrating the benefit of allowing for nonlinear effects. These findings show that the two types of vocalizations are influenced by speed and breathing rate in a very different manner, thus supporting the hypothesis that they are produced by distinct physiological mechanisms, and may play distinct behavioural roles.

As explained in Section 2.8, we fitted additional models, restricted to the encounter phase, with an interaction between state and body orientation, to assess if angle was associated with vocalization within any of the three during-encounter states. The most prominent of the state-specific angle effects displayed in Table 4 is a negative effect on USV count while the subject is touching the social stimulus ($p = 3.5 \times 10^{-7}$). This implies that USVs occur more while the subject rat is touching and turned toward the stimulus rat. The same message can be gleaned from the density estimates of body angle toward the social stimulus in Fig. 5, given separately for half-seconds with one or more USVs, those with one or more LFVs, and those with no vocalization. The body angle distribution is seen to be shifted to the left (orientation toward the stimulus rat) during half-seconds with USVs.

3.4. Spatial and temporal association with social interaction

Our results so far suggest distinct mechanisms and roles for USVs and LFVs, with the former associated with social interaction. To further explore this possibility, we analyzed the spatial distribution of USV and LFV emissions during the encounter, relative to the chamber of the social stimulus. As depicted in Fig. 6A, almost all USVs were emitted near the chamber of the social stimulus. In contrast, LFV emissions (Fig. 6B) showed a much wider spatial distribution, which resembled the distribution of the subject locations (Fig. 6C). Moreover, when calculating the distance from the social chamber for the location of each emission, we found a significant difference between the two vocalization types: while USVs were emitted almost exclusively near the social stimulus chamber, LFVs were emitted also in more distant locations (Fig. 6D). Finally, we examined the likelihood that each of the three types of vocalization recorded (subject USV, stimulus USV and subject LFV) would occur within five seconds (co-occurrence) from a vocalization of the other type, we found that the only type of temporal association that was statistically significant relative to shuffled data was when a stimulus USV co-occurred with subject USV (Fig. 6E). Together, these results suggest that subject USVs are both temporally and spatially associated with interaction with the social stimulus, while no such association was found

Table 2
Performance metrics for LFV and USV detection from breathing patterns using an LSTM-CNN model. The model achieved high performance for USV detection (F1 = 0.744), indicating that USVs are tightly linked to significant changes in the breathing waveform, whereas the same model struggled to distinguish LFV cycles from SB cycles (F1 = 0. 394). The low precision for LFV prediction (0.324) reflects the high rate of false positives, consistent with our observation that LFV-bearing cycles differ only subtly from SB cycles.

Metric	USV	LFV
True positives (TP)	444	71
False positives (FP)	232	148
True negatives (TN)	13650	14111
False negatives (FN)	74	70
Precision	0.657	0.324
Recall	0.857	0.504
F1 score	0.744	0.394

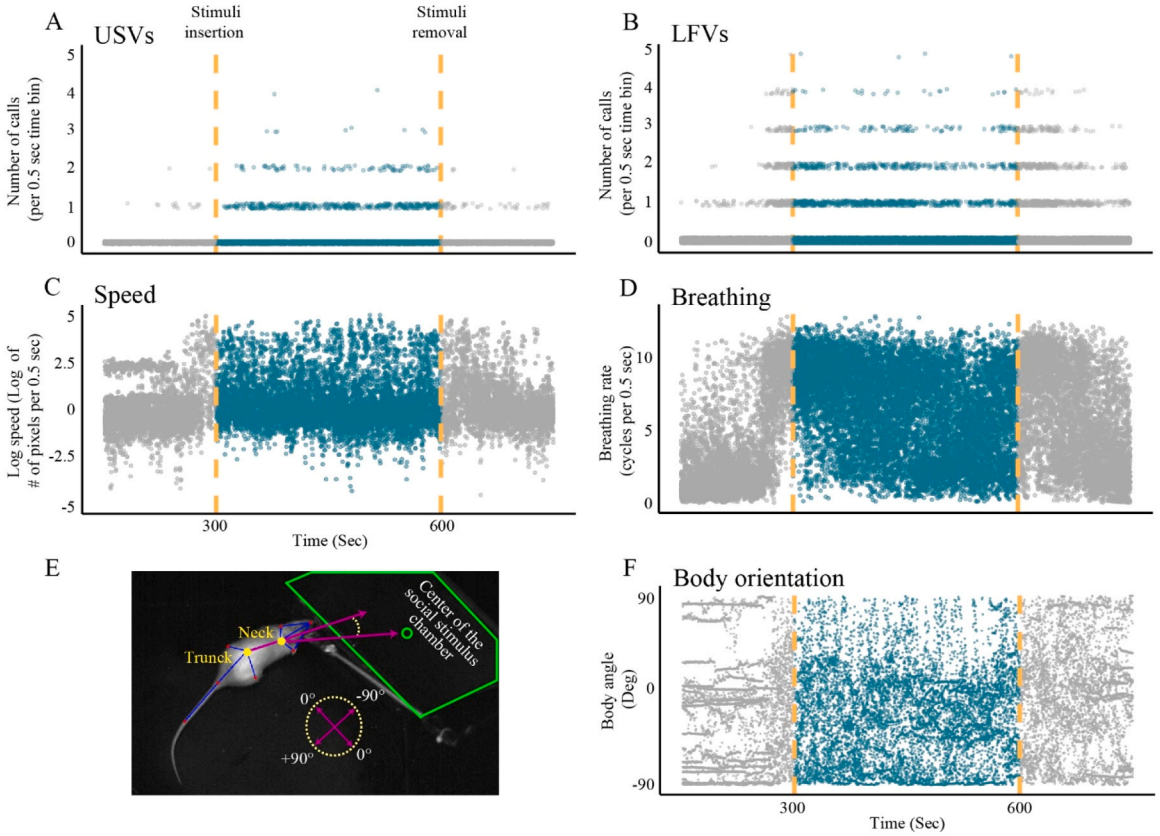

Fig. 3. Variables of interest plotted against time. Each of these plots displays the values of a variable of interest in each half-second interval, for all trials pooled together. Grey points denote events during the pre- and post-encounter phases (without social interaction), while turquoise points denote events during the encounter period (from 300 to 600 s), when social interaction occurred (stimulus rat present). (A) Number of USVs. (B) Number of LFVs. (C) Log of speed. (D) Breathing rate (0.5 Hz). (E) Schematic presentation of the body angle relative to stimulus chamber. (F) Angle of body orientation (degrees; see Section 2.5.2).

Table 3
Parameter estimates for the negative binomial models for USVs and LFVs.

	USV		LFV	
Regression coefficient	Estimate	p-value	Estimate	p-value
Intercept	−7.68	–	−3.496	–
Touching social stimulus during encounter	2.827	$< 2 \times 10^{-16}$ ***	−0.020	0.826
Touching object during encounter	1.335	0.02 *	0.357	0.048*
Touching neither during encounter	2.778	$< 2 \times 10^{-16}$ ***	−0.306	0.008**
Post-encounter	1.347	7.78×10^{-6} ***	0.174	0.084
Estimate of θ (negative binomial parameter)	2.217		0.39	

for the LFVs.

Since LFVs were not found to be associated with social interaction, we hypothesized that they may be linked to the arousal/alertness state of the animal. In rats, arousal is known to be associated with elevation of breathing rate from < 5 Hz to to 5–20 Hz and increased theta rhythmicity in limbic areas associated with emotions, such as the nucleus accumbens. Therefore, we examined the temporal pattern of LFV and USV rate along the experiment, with the breathing rate of the same animals. We also compared these variables with theta rhythmicity of local field potentials recorded from the nucleus accumbens core (AcbC) of a different group of rats performing the same type of experiment. As shown in Fig. 7, LFP theta power, breathing rate and LFV rate were all induced about 50 s before the introduction of the stimuli to the arena (likely triggered by preparation for stimuli introduction), peaked just before the insertion, and then decayed till the end of the social encounter, where another peak was induced near the removal of the stimuli from the arena. This common temporal pattern of all three variables fits with high arousal/alertness states during the insertion and removal of the stimuli to the arena. In contrast, USV rate was elevated only after stimuli introduction, most probably as part of interactions with the social stimulus. Overall, these results further suggest that the LFVs are associated with the arousal state of the animal, while USVs are linked to social interactions.

4. Discussion

Animal vocalizations may be intential and meaningful, like functional referential calls, or may carry information about the individual's affect, either by being driven by it or because their characteristics change by the individual's internal state. Notably, increasing evidence suggests that this distinction is not dichotomous, as many animal vocalizations simultaneously convey information about both external events and the emotional state of the caller (for a recent review article, see [1]). Thus, rather than representing separate categories, referential and affective vocalizations may be viewed as endpoints along a continuum of communicative signals that differ in the relative contribution

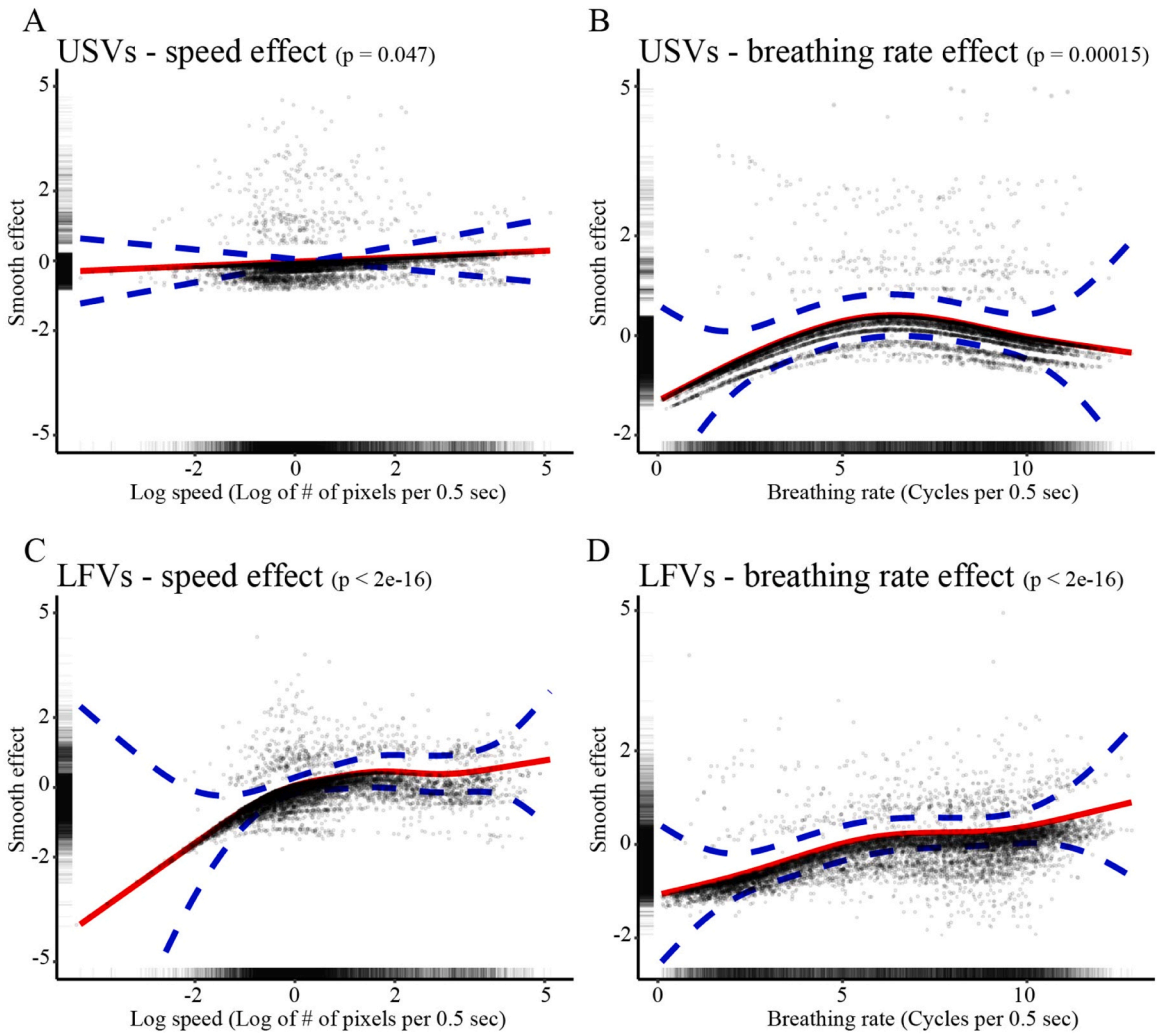

Fig. 4. Smooth nonlinear effects (f_1, f_2) of log speed and breathing rate, respectively, on counts of USVs (A, B) and LFVs (C,D). Function estimates are shown in red and 95% pointwise confidence intervals in blue.

Table 4
Effect of body angle on USVs and LFVs, within each of the during-encounter states. Here a negative effect indicates more vocalizations when turned toward the stimulus rat.

	USV		LFV	
While touching…	Estimate	p-value	Estimate	p-value
Social	−0.0088	3.5×10^{-7}	0.0042	0.0054
Object	0.0045	0.80	−0.0041	0.34
Neither	−0.0035	0.85	0.0016	0.39

of social meaning and emotional expression. Our study focused on the distinct respiratory mechanisms and functional roles of two different types of rat vocalizations: USVs and LFVs. Our findings suggest that these two vocalization types may be differentially related to the individual's social behavior and internal state.

4.1. Vocalizations and breathing patterns

Our results demonstrate that USVs and LFVs are associated with distinct phases of the respiratory cycle, underscoring their differing production mechanisms. In agreement with a previous study [17], we found that USVs are coupled to early exhalation stages and are consistently accompanied by a secondary elevation—or "second hump"—in the exhalation waveform. This feature likely reflects active modulation of expiratory airflow and subglottal pressure, required to sustain ultrasonic vocal output [32]. In contrast, LFVs occur reliably during the early stage of inhalation and are accompanied by relatively smooth breathing waveforms that closely resemble spontaneous breathing, although the quantitative analyses revealed small differences between LFV and SB cycles. These qualitative differences were evident in average cycle morphology (Fig. 2E-G), and were also reflected in the durations of breathing cycles: USV cycles were significantly longer than SB cycles, which were slightly but significantly longer than LFV cycles (Fig. 2D). Moreover, DTW distances from the SB template were substantially greater for USV cycles than for LFV cycles. LFV cycles also showed slightly greater DTW distances than SB cycles, indicating that LFVs are associated with subtle changes in the respiratory trajectory, although these changes are much smaller than those associated with USVs. We further analyzed the timing of vocalization peak phases using circular statistics. USV peak clustered around early exhalation, whereas LFV peaks were grouped in the first half of inhalation (Fig. 2C). Together, these findings reinforce that USVs and LFVs are temporally dissociated within the breathing cycle and differ in the degree and nature of their respiratory modulation. Their occurrence during opposite phases of respiration, together with their distinct breathing trajectories, supports the conclusion that they are generated through different physiological mechanisms.

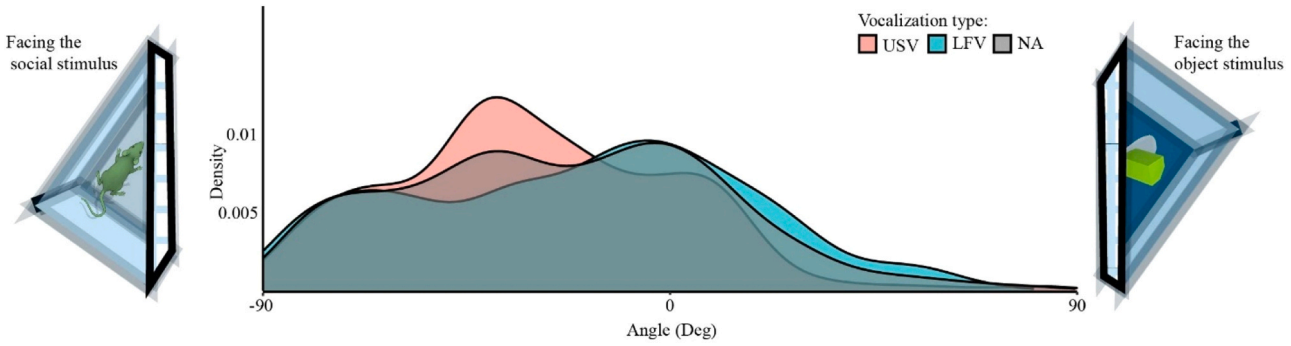

Fig. 5. Distribution of body angle during half-seconds with USVs, with LFVs, and with neither.

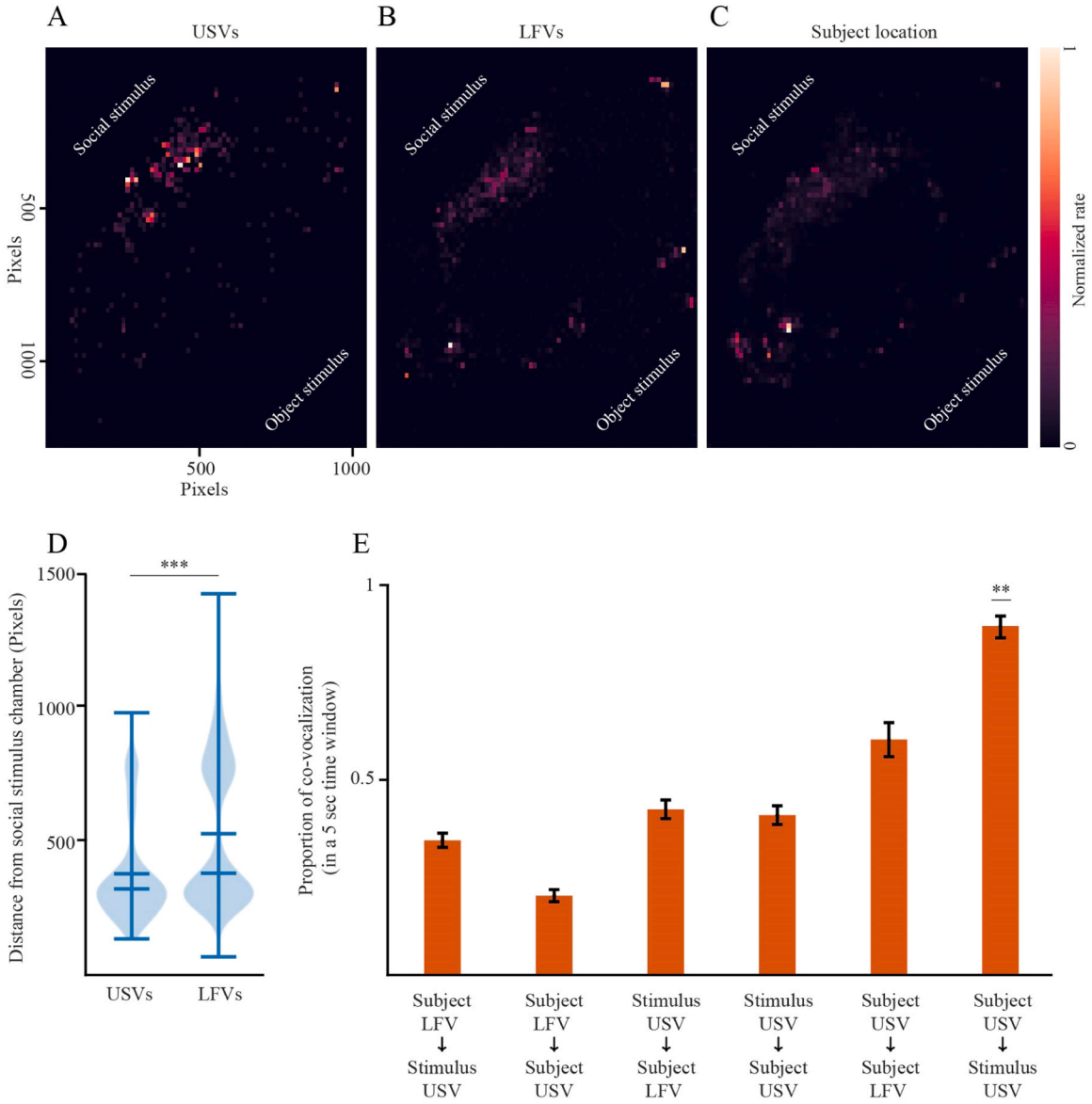

Fig. 6. Spatial distribution of vocalizations and cross-vocalization probabilities. (A-C) Spatial heat maps showing locations of subject USVs (A), subject LFVs (B), and overall subject occupancy in the arena (C). Warmer colors indicate higher normalized rates. The social stimulus is aligned to the upper-left corner across sessions, and the object stimulus appears in the opposite corner. (D) Distribution of distances from the social chamber centroid for USVs and LFVs. LFVs were emitted significantly farther from the social stimulus, as compared to USVs (*** $p < 0.001$). (E) Pooled probabilities of a vocalization of a given type to be detected within the 5-s time window around a reference call for all ordered call pairs. Error bars denote variability estimated across all calls. Significant deviations from the circular-shift surrogate distribution are indicated (**, see Methods).

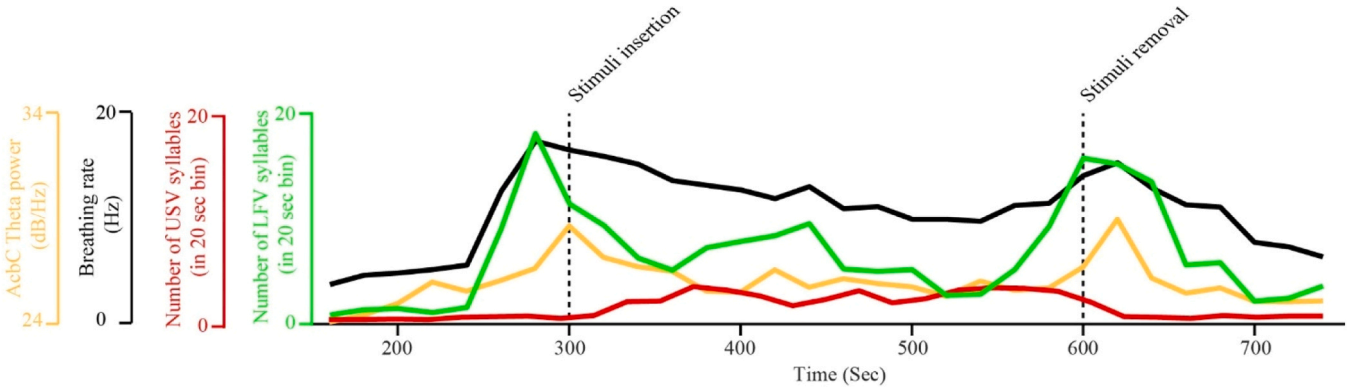

Fig. 7. Dynamics of AcbC LFP theta power (yellow), Breathing rate (black), number of USVs (Red) and number of LFVs (green), all averaged across recorded sessions in 20-s bins along the social preference experiment. Note that theta power was recorded in a different group of animals while all other variables were recorded from the same group of animals. Time points of stimuli insertion and removal are denoted by dashed lines.

4.2. Detection of vocalizations using breathing patterns and locomotion

The distinction between the two vocalization types is further supported by the difference in the ability to predict their emission using the breathing pattern. A convolutional neural network model demonstrated high accuracy in detecting USVs from the breathing pattern, reflecting the significant deviations in breathing patterns associated with these vocalizations. However, the same approach failed to reliably detect LFVs, likely because the respiratory changes associated with LFVs were small relative to the variability and overlap between individual LFV and SB cycles. This discrepancy indicates that LFVs have minimal effect on the respiratory rhythm, implying limited active modulation of respiratory mechanics relative to USVs. On the other hand, the semiparametric mixed-effects model associated LFVs with the combined effect of breathing and movement, unlike USVs, which are less influenced by movement. It should be noted that a previous study [33] found interaction among the type of rat movement (walking, trotting or galloping), USV rate and its coupling to respiration. In our study, however, the restricted size of the arena allowed only walking, which may explain the lack of interaction with speed. Taken together, these results suggest that the two vocalization types are driven by distinct physiological mechanisms. Moreover, the strong association of USVs with social behavior, together with their pronounced and consistent respiratory modulation, is consistent with their role as socially directed vocal signals. In contrast, LFVs, which may be described as a form of "heavy breathing," appear to be more closely associated with the individual's internal physiological or arousal state.

4.3. Distinctions between USVs and LFVs in behavioral contexts

We found USVs to be emitted almost exclusively during the social encounter phase of the experiment, aligning with previous research linking them to mating, play, and other social behaviors [18]. Moreover, the semiparametric mixed model showed a strong association of USVs, but not LFVs, with body angle toward the social stimulus during the encounter (Fig. 5). We also found that USVs are emitted almost solely near the social stimulus and show significant co-occurrence with the USVs emitted by the stimulus (Fig. 6). In contrast, LFVs were elicited about 50 s before the social encounter phase, in parallel to the rise in active breathing rate, which we speculate reflects the arousal state induced by the experimenter's preparations for stimuli introduction. Moreover, both LFV and breathing rate peaked around the insertion of the stimuli to the arena and their removal from there, thus creating a temporal pattern very similar to theta rhythmicity of LFP signals recorded from the nucleus accumbens (Fig. 7). We previously showed that such increase in theta rhythmicity is widely observed in brain limbic areas associated with affective states and are likely to reflect the arousal state of the animal [34]. This suggests that LFVs are more closely associated with general arousal state, which has a positive relationship with movement and locomotion [35,36]. Accordingly, the semi-parametric mixed models revealed that speed was associated significantly with LFVs but minimally with USVs, further supporting the hypothesis that LFVs are tied to broader physiological or behavioral states rather than specific events of social interaction.

Overall, our findings are consistent with the established role of USVs as intentional communicative signals in rats, linked to specific social behaviors and requiring complex respiratory modulation for production. LFVs, by contrast, appear to reflect an internal state, likely related to arousal/alertness or other general physiological processes. The temporal separation between LFVs and USVs within the breathing cycle, with LFVs peaking during early inhalation and USVs during early exhalation (Fig. 2C), underscores their distinct functional roles and production mechanisms.

4.4. The functional role of LFVs

The functional nature of LFVs, whether they represent a communicative signal or a strictly physiological by-product, remains an open question. Several findings from our study suggest that LFVs may be a passive consequence of heightened arousal or rapid breathing. Their occurrence during the early stages of inhalation and their relatively subtle respiratory signature point to a physiological origin that may be strongly influenced by airflow dynamics, rather than the pronounced respiratory modulation observed during USV production. Furthermore, their weak associations with social behavior contrast with the intentional and social nature of USVs, which are tightly linked to social interaction.

Nevertheless, parallels with neonatal rodent USVs are worth considering. These calls, produced primarily during cold stress, are well-documented as acoustic by-products of laryngeal braking, a thermoregulatory mechanism during respiration [37,38]. Despite this, pup USVs serve an unequivocally social role, eliciting parental retrieval and caregiving behaviors [37,39]. Therefore, even sounds that originate as incidental by-products of breathing can later be co-opted and used as purposeful social signals [37,40], similarly to sighs in humans. The dual nature of pup USVs - physiological by-products and critical social signals - suggests a possible analogy to LFVs. While LFVs may arise incidentally during heavy breathing, they could nonetheless carry social information about arousal or physiological states, influencing group dynamics or conspecific behaviors in subtle ways. While LFVs were too weak to be clearly detected by the arena microphone, which may make their detection by other conspecifics questionable, a recent study demonstrated that mice can detect and respond to very weak noises, such as the rubbing of a whisker against an object [41]. Thus, despite being weak,

LFVs may be detected by nearby rats. Future research should explore whether LFVs, like pup USVs, elicit responses from conspecifics; this may reveal whether these vocalizations play an adaptive communicative role [18,42].

4.5. Limitations

Several limitations of our study should be noted. First, the semi-parametric models reported here sought to relate USV and LFV counts, within each half-second bin, with several variables related to the subject rat's movement, breathing, and position with respect to the stimulus rat. While the results are consistent with our general conclusion that USVs are more related to social interaction while LFVs reflect arousal, it must be acknowledged that by their nature, such regression models can only highlight associations among the measured variables, rather than revealing underlying physiological mechanisms. Second, while the differences between LFV and SB cycles were statistically significant in both the duration and DTW analyses, their magnitudes were small. Therefore, the physiological importance of these differences should be interpreted cautiously, particularly given the large number of breathing cycles included in the analyses. Third, while our results indirectly suggest distinct physiological mechanisms of the two vocalization types, we did not examine these mechanisms directly. Finally, we did not check whether LFVs appear in other non-social high-arousal states or whether they are limited to social interactions.

4.6. Summary

Using long short-term memory convolutional neural networks and semiparametric mixed-effects models, we have analysed here the interplay among two types of rat vocalizations, respiration, and movement during social interactions. These analyses demonstrate that USVs and LFVs represent distinct physiological phenomena, with USVs closely tied to social dynamics and LFVs reflecting an internal state. These findings advance the understanding of rodent vocal communication and suggest a potential adaptive role of LFVs in behavioural contexts.

CRediT authorship contribution statement

Yizhaq Goussha: Writing – original draft, Visualization, Software, Methodology, Formal analysis, Conceptualization. **Noemi Foà:** Writing – original draft, Visualization, Software, Methodology, Formal analysis, Conceptualization. **Shai Netser:** Writing – review & editing, Validation, Project administration, Methodology, Data curation, Conceptualization. **Philip Tzvi Reiss:** Writing – review & editing, Supervision, Methodology, Formal analysis, Conceptualization. **Rishika Tiwari:** Investigation. **Shanah Rachel John:** Methodology, Investigation. **Shlomo Wagner:** Writing – review & editing, Supervision, Funding acquisition, Conceptualization.

Appendix A. Supporting information

Supplementary data associated with this article can be found in the online version at doi:10.1016/j.bbr.2026.116417.

Data and code availability

All codes and processed data used for this paper are available in Zenodo (https://doi.org/10.5281/zenodo.20374529).

References

[1] T. Gruber, et al., Emotion in nonverbal communication: comparing animal and human vocalizations and human text messages', Emot. Rev. 17 (1) (2025) 30–45.
[2] R.M. Seyfarth, D.L. Cheney, Meaning and Emotion in animal vocalizations, Ann. N. Y. Acad. Sci. 1000 (1) (2003) 32–55, https://doi.org/10.1196/ANNALS.1280.004.
[3] R.M. Seyfarth, D.L. Cheney, P. Marler, Vervet monkey alarm calls: Semantic communication in a free-ranging primate, Anim. Behav. 28 (4) (1980) 1070–1094, https://doi.org/10.1016/S0003-3472(80)80097-2.
[4] R.M. Seyfarth, D.L. Cheney, Signalers and receivers in animal communication, Annu. Rev. Psychol. 54 (2003) 145–173, https://doi.org/10.1146/annurev.psych.54.101601.145121.
[5] E.F. Briefer, Vocal contagion of emotions in non-human animals', Proc. R. Soc. B Biol. Sci. 285 (1873) (2018) https://doi.org/10.1098/RSPB.2017.2783/78840.
[6] E.F. Briefer, S. Le Comber, Vocal expression of emotions in mammals: mechanisms of production and evidence, J. Zool. 288 (1) (2012) 1–20, https://doi.org/10.1111/J.1469-7998.2012.00920.X.
[7] M. Wöhr, R.K.W. Schwarting, Ultrasonic communication in rats: Can playback of 50-kHz calls induce approach behavior? PLOS One 2 (12) (2007) https://doi.org/10.1371/JOURNAL.PONE.0001365.
[8] S.M. Brudzynski, Ultrasonic calls of rats as indicator variables of negative or positive states: Acetylcholine-dopamine interaction and acoustic coding, Behav. Brain Res. 182 (2) (2007) 261–273, https://doi.org/10.1016/j.bbr.2007.03.004.
[9] J. Burgdorf, R.A. Kroes, J.R. Moskal, J.G. Pfaus, S.M. Brudzynski, J. Panksepp, Ultrasonic vocalizations of rats (Rattus norvegicus) during mating, play, and aggression: Behavioral concomitants, relationship to reward, and self-administration of playback, J. Comp. Psychol. 122 (4) (2008) 357–367, https://doi.org/10.1037/A0012889.
[10] J.P. Neunuebel, A.L. Taylor, B.J. Arthur, S.E. Roian Egnor, Female mice ultrasonically interact with males during courtship displays (no. MAY), Elife 4 (2015) 1–24, https://doi.org/10.7554/ELIFE.06203.
[11] J.S. Burgdorf, S.M. Brudzynski, J.R. Moskal, Using rat ultrasonic vocalization to study the neurobiology of emotion: from basic science to the development of novel therapeutics for affective disorders, Curr. Opin. Neurobiol. 60 (2020) 192–200, https://doi.org/10.1016/J.CONB.2019.12.008.
[12] D.W. Wesson, Sniffing behavior communicates social hierarchy, Curr. Biol. 23 (7) (2013) 575–580, https://doi.org/10.1016/J.CUB.2013.02.012.
[13] A. Kurnikova, J.D. Moore, S.M. Liao, M. Deschênes, D. Kleinfeld, Coordination of orofacial motor actions into exploratory behavior by rat, Curr. Biol. 27 (5) (2017) 688–696, https://doi.org/10.1016/J.CUB.2017.01.013.
[14] D. Kleinfeld, M. Deschênes, N. Ulanovsky, Whisking, sniffing, and the hippocampal θ-rhythm: A tale of two oscillators, PLoS. Biol. 14 (2) (2016), https://doi.org/10.1371/JOURNAL.PBIO.1002385.
[15] M.M. Kabir, M.I. Beig, M. Baumert, M. Trombini, F. Mastorci, A. Sgoifo, F. R. Walker, T.A. Day, E. Nalivaiko, Respiratory pattern in awake rats: Effects of motor activity and of alerting stimuli, Physiol. Behav. 101 (1) (2010) 22–31, https://doi.org/10.1016/J.PHYSBEH.2010.04.004.
[16] T. Riede, C. Schaefer, A. Stein, Role of deep breaths in ultrasonic vocal production of Sprague-Dawley rats, J. Neurophysiol. 123 (3) (2020) 966, https://doi.org/10.1152/JN.00590.2019.
[17] Y.B. Sirotin, M.E. Costa, D.A. Laplagne, Rodent ultrasonic vocalizations are bound to active sniffing behavior' (no. NOV), Front. Behav. Neurosci. 8 (2014) 107287.
[18] S.R. John, R. Tiwari, Y. Goussha, R. Amar, A. Bizer, S. Netser, S. Wagner, Simultaneous recording of ultrasonic vocalizations and sniffing from socially interacting individual rats using a miniature microphone, Cell. Rep. Methods 3 (11) (2023) 100638, https://doi.org/10.1016/j.crmeth.2023.100638.
[19] S.N. Wood, N. Pya, B. Säfken, Smoothing parameter and model selection for general smooth models, J. Am. Stat. Assoc. 111 (2016) 1548–1563, https://doi.org/10.1080/01621459.2016.1180986.
[20] S. Netser, S. Haskal, H. Magalnik, A. Bizer, S. Wagner, A system for tracking the dynamics of social preference behavior in small rodents, J. Vis. Exp. 2019 (153) (2019), https://doi.org/10.3791/60336.
[21] R. Tiwari, S. Raz, S. Netser, S. Wagner, Oxytocin-dependent reorganization of social vs. food motivational hierarchy and corticostriatal neural activity by social isolation in rats', 2026.01.19.700365, bioRxiv (2026), https://doi.org/10.64898/2026.01.19.700365.
[22] S.R. John, W. Dagash, A.N. Mohapatra, S. Netser, S. Wagner, Distinct dynamics of theta and gamma rhythmicity during social interaction suggest differential mode of action in the medial amygdala of sprague dawley rats and C57BL/6J Mice, Neuroscience 493 (Jun. 2022) 69–80, https://doi.org/10.1016/J.NEUROSCIENCE.2022.04.020.
[23] A. Mathis, et al., DeepLabCut: markerless pose estimation of user-defined body parts with deep learning, vol. 21, no. 9, Nat. Neurosci. 21 (9) (2018) 1281–1289, https://doi.org/10.1038/s41593-018-0209-y.
[24] Y. Goussha, K. Bar, S. Netser, L. Cohen, Y. Hel-Or, S. Wagner, HybridMouse: a hybrid convolutional-recurrent neural network-based model for identification of mouse ultrasonic vocalizations, Front. Behav. Neurosci. 15 (2022) 810590, https://doi.org/10.3389/FNBEH.2021.810590/BIBTEX.
[25] N. Otsu, Threshold selection method from gray-level histograms, IEEE Trans. Syst. Man. Cybern. SMC-9 (1) (1979) 62–66, https://doi.org/10.1109/TSMC.1979.4310076.
[26] M. Müller, Fundamentals on music and audio data. Information Retrieval for Music and Motion, Springer, Berlin, Heidelberg, 2007, pp. 17–50, https://doi.org/10.1007/978-3-540-74048-3_2.
[27] H. Sakoe, S. Chiba, Dynamic programming algorithm optimization for spoken word recognition, IEEE Trans. Acoust. 26 (1) (1978) 43–49, https://doi.org/10.1109/TASSP.1978.1163055.
[28] K.V. Mardia, P.E. Jupp, Directional Statistics, Wiley, 2000, https://doi.org/10.1002/9780470316979.
[29] K. He, X. Zhang, S. Ren, and J. Sun, 'Deep residual learning for image recognition', 2016. Accessed: Apr. 30, 2025. [Online].

[30] S.N. Wood. Generalized Additive Models: An Introduction With R, (2nd ed.), CRC Press, 2017.
[31] M. Fasiolo, R. Nedellec, Y. Goude, S.N. Wood, Scalable visualization methods for modern generalized additive models, J. Comput. Graph. Stat. 29 (1) (2020) 78–86.
[32] L.H. Roberts, Correlation of respiration and ultrasound production in rodents and bats, J. Zool. 168 (4) (1972) 439–449, https://doi.org/10.1111/J.1469-7998.1972.TB01360.X.
[33] J.A. Alves, B.C. Boerner, D.A. Laplagne, Flexible coupling of respiration and vocalizations with locomotion and head movements in the freely behaving rat, Neural Plast. 2016 (1) (2016) 4065073, https://doi.org/10.1155/2016/4065073.
[34] A. Tendler, S. Wagner, Different types of theta rhythmicity are induced by social and fearful stimuli in a network associated with social memory, Elife 4 (4) (2015), https://doi.org/10.7554/ELIFE.03614.
[35] R.S. Larsen, J. Waters, Neuromodulatory correlates of pupil dilation, Front. Neural Circuits 12 (2018) 309004, https://doi.org/10.3389/FNCIR.2018.00021/BIBTEX.
[36] M. Vinck, R. Batista-Brito, U. Knoblich, J.A. Cardin, Arousal and locomotion make distinct contributions to cortical activity patterns and visual encoding, Neuron 86 (2015) 740–754, https://doi.org/10.1016/j.neuron.2015.03.028.
[37] M.S. Blumberg, J.R. Alberts, Ultrasonic vocalizations by rat pups in the cold: an acoustic by-product of laryngeal braking? Behav. Neurosci. 104 (5) (1990) 808–817, https://doi.org/10.1037/0735-7044.104.5.808.
[38] M.A. Hofer, H.N. Shair, Ultrasonic vocalization, laryngeal braking, and thermogenesis in rat pups: a reappraisal, Behav. Neurosci. 107 (2) (1993) 354–362, https://doi.org/10.1037/0735-7044.107.2.354.
[39] M.A. Hofer, Multiple regulators of ultrasonic vocalization in the infant rat, Psychoneuroendocrinology 21 (2) (1996) 203–217, https://doi.org/10.1016/0306-4530(95)00042-9.
[40] B.H. Blake, Ultrasonic vocalization and body temperature maintenance in infant voles of three species (Rodentia: Arvicolidae), Dev. Psychobiol. 25 (8) (1992) 581–596, https://doi.org/10.1002/DEV.420250805.
[41] B. Efron, A. Ntelezos, Y. Katz, I. Lampl, Detection and neural encoding of whisker-generated sounds in mice, Curr. Biol. 35 (6) (2025) 1211–1226.e8, https://doi.org/10.1016/j.cub.2025.01.061.
[42] L.A. Geyer, Olfactory and thermal influences on ultrasonic vocalization during development in rodents, Integr. Comp. Biol. 19 (2) (1979) 419–431, https://doi.org/10.1093/ICB/19.2.419.